ISSN (Print) 1226-1750
ISSN (Online) 2233-6656
Journal of Magnetics 24(2), 286-293 (2019) https://doi.org/10.4283/JMAG.2019.24.2.286

Variations in The Apparent Diffusion Coefficient Based on The Number of Applied B-Values in Brain Parenchymal Tissue on Diffusion Weighted Magnetic Resonance Imaging

Sung Jin Kang and A Leum Lee*

Department of Radiology, Soonchunhyang University Bucheon Hospital, Bucheon 14584, Republic of Korea

(Received 21 January 2019, Received in final form 11 April 2019, Accepted 11 April 2019)

The purpose of this study was to investigate the changes in apparent diffusion coefficient of brain parenchymal tissue according to the number of application of b-values in diffusion weighted images. The diffusion weighted image was obtained from 13 subjects using 3.0 Tesla MRI scanner. At this time, each ADC map image was created after obtaining the image by dividing it into the method for applying b-values 0, 1,000 and b-values 0, 500, 1,000 and 1,500 respectively. To quantitatively compare the ADC values, two observers measured the mean ADC values by setting four ROIs in each white matter, gray matter, thalamus, globus pallidus in the ADC map images. The ADC values measured from the two methods were validated with statistical analysis tools. In the two imaging methods, the inter-observer reliability of the measured ADC values is analyzed by using the ICC, there was a good correlation and a significant difference in white matter, thalamus and the globus pallidus excluding gray matter ($p < 0.05$). Also, Mann Whitney U test are used to verify statistical Results of significance verification of ADC values changes in the intra-observer, Observers 1 were significant in all ROIs between the two methods ($p < 0.05$). Observers 2 were significant in the white matter, thalamus and globus pallidus ($p < 0.05$). However, Gray matter was unable to identify significant results ($p > 0.05$). As a results, the variation of the ADC values according to the number of applying of b-values in a brain parenchyma usually is statistically significant. So, since the ADC value of the brain parenchyma tissue is a relative value for various conditions, it is necessary to apply it considering the time required for imaging and the characteristics of the brain disease rather than necessarily applying a large number of b-value sampling.

Keywords : MRI (magnetic resonance imaging), DWI (diffusion weighted image), ADC (apparent diffusion coefficient)

1. Introduction

Diffusion is a microscopic and irregular movement of molecules within matter. Diffusion-weighted magnetic resonance imaging (DW-MRI) uses the diffusion of water molecules *in vivo* to generate images with different degrees of water molecular diffusion in human tissues. Based on the resulting images, presented as signal intensity, DWI allows for the quantification of tissue characteristics [1]. However, in reality, the diffusion of water molecule inside a human body is often hindered by cell membrane or large protein molecules, and therefore complete diffusion does not occur. Thus, the diffusion coefficient measured in DW-MRI reflects restricted diffusion caused by several factors, which is also known as the apparent diffusion coefficient (ADC). To measure ADC of a specific tissue, at least two different b-values need to be applied to obtain DW-MRI images. The slope of a graph showing the relationship of signal intensities of the images versus b-values represents the ADC for the tissue. Furthermore, an ADC map, where the resulting ADC values are computed on a pixel-by-pixel basis, can be created. Utilizing this ADC map image, diffusion characteristics of individual tissues in the human body or pathological changes can be represented in a more quantitative manner [4, 5].

Currently, the ADC maps at most clinical institutions are obtained from two different b-values, 0 and 1,000, in the diffusion-weighted imaging of the brain. However, the calculation of an ADC value based on the mono-exponential decay pattern using two b-values may not accurately represent the actual ADC value that reflects restricted diffusion occurring in the human body. For these reasons,

*Corresponding author: Tel: +82-32-621-6559
Fax: +82-32-621-5874, e-mail: aleerad@schmc.ac.kr

some previous studies have reported the usefulness of the calculated ADC value from at least three b-values in abdominal organs [6, 7]. Therefore, this study aims to examine the ADC variation set multiple b-values, especially in comparison with ADC values measured in the brain parenchyma, where two different b-values are typically used for the measurement.

2. Subjects and Methods

2.1. Research subjects

This retrospective study was approved with a waiver of informed consent by our Institutional Review Board (SCHBC 2019-01-009-001).

Of the patients who underwent brain MRI at OO university hospital (Gyeonggi-do, South Korea) between July and August, 2018 for a primary complaint of neurologic symptoms, 13 patients (8 males and 5 females) within normal limits were included in this study.

2.2. Research methods

For all subjects, 3.0 Tesla MRI (MAGNETOM Skyra, SIEMENS, Erlangen, Germany) and RF coil for head and neck examination (Head/Neck 64 channel coil, SIEMENS, Erlangen, Germany) were utilized to obtain images. For obtaining DW-MRI images, spin echo-echo planar imaging (SE-EPI) pulse sequence method was utilized. The cross-sectional image was aligned parallel to the virtual line connecting the anterior and posterior commissure, and the images were taken in the direction from the base to the vertex of the brain.

In order to measure the changes in ADC value based on the number of times b-value is used, the following imaging techniques were employed: First is the conventional method to obtain brain DW-MRI (hereinafter referred to as '**$ADC_{2\ b\text{-}value}$**') utilizing two b-values of 0 and 1,000 (unit: s/mm^2) ; Second is the method proposed in this study (hereinafter referred to as '**$ADC_{4\ b\text{-}value}$**') utilizing four b-values of 0, 500, 1,000, and 1,500. The resulting images were then used to create the ADC maps respectively.

In the '**$ADC_{2\ b\text{-}value}$**' method, the ADC values can be calculated using Equation (1) as follows.

$$\mathrm{ADC} = -\ln(SI_{b0}/SI_{b1000})/(b_0 - b_{1000}) \quad (1)$$

Where SI_{b0} and SI_{b1000} represent the signal intensities for the corresponding b-values.

For the ADC calculation in the '**$ADC_{4\ b\text{-}value}$**' method, Equation (2) was used as shown below.

$$\mathrm{ADC} = N\sum_{i=1}^{N} biSI - \sum_{i=1}^{N} bi \sum_{i=1}^{N} SI/N\sum_{i=1}^{N} bi^2 - \left(\sum_{i=1}^{N} bi\right)^2 \quad (2)$$

Where N represents the number of b-values used, b represents the b-value, and SI represents the signal intensity.

The image acquisition parameters were set as follows: repetition time (TR) /echo time (TE) of 5370/73 ms, slice thickness/spacing of 5/1 mm, field of view (FOV) of 220 × 220 mm, imaging matrix size of 192 × 192, number of excitation (NEX) per b-value of 1, parallel imaging factor of 2, and diffusion gradient magnetic field in 3 different directions. The scan times for $ADC_{2\ b\text{-}value}$ and $ADC_{4\ b\text{-}value}$ methods were 110 and 280 second, respectively.

For quantitative comparison of ADC values, the mean ADC value (unit: 10^{-3} mm^2/s) was measured within four separate regions of interest (ROI) selected independently by two observers using the images taken with the $ADC_{2\ b\text{-}value}$ and $ADC_{4\ b\text{-}value}$ methods. These four ROIs only contain the brain parenchyma such as gray and white matter in the frontal lobe, thalamus, and globus pallidus. Conventional T2-weighted image obtained at the same spatial location, for the accurate ROI determination, was consulted to ensure that the location and surface area of the ROIs are maintained unchanged for the brain paren-

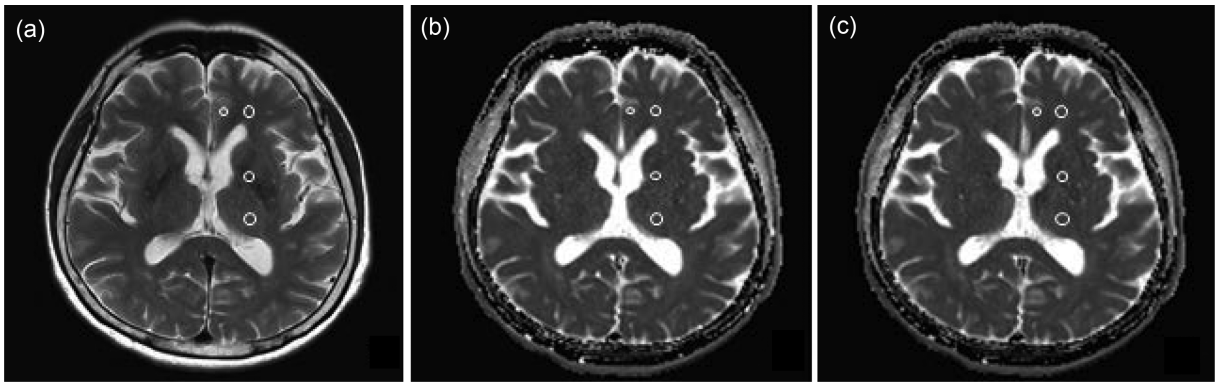

Fig. 1. MR image shows ROIs were set at locations of white matter, gray matter, thalamus and globus pallidus on T2 weighted image (a), $ADC_{2\ b\text{-}value}$ image (b) and $ADC_{4\ b\text{-}value}$ image (c) respectively.

chyma across the $ADC_{2\ b\text{-}value}$ and $ADC_{4\ b\text{-}value}$ images (Fig. 1).

All images were analyzed with an image analysis software (syngo.via Client 4.1, SIEMENS, Germany).

2.3. Statistical analysis

For quantitative analysis, statistical significance tests were conducted on the measured values for each ROI from the $ADC_{2\ b\text{-}value}$ and $ADC_{4\ b\text{-}value}$ images.

First, to assess the inter-observer reliability of the ADC values measured by two observers, a significance test of correlation was performed using the intra-class correlation coefficient (ICC) on the measured ADC values from the $ADC_{2\ b\text{-}value}$ and $ADC_{4\ b\text{-}value}$ images. The correlation coefficient was measured on the following scale: poor for the ICC values less than 0.4; fair for values between 0.4-0.59; good for values between 0.6-0.74; and excellent for values between 0.75-1.0. Moreover, Mann Whitney U test was utilized to determine the statistical significance of the intra-observer variation in the measured ADC value based on the two different imaging techniques, namely $ADC_{2\ b\text{-}value}$ and $ADC_{4\ b\text{-}value}$ methods.

Statistical analyses were performed using SPSS(ver. 25.0, KoreaPlus Statistic for Medical Service, SPSS Inc.), and the results with a *p*-level of 0.05 or less were considered statistically significant.

3. Results

3.1. General characteristics of the subjects

The age of the subjects ranged from 39 to 63 years, with a mean age of 48.57 ± 12.06 years for males and 54.24 ± 9.12 for females.

3.2. Observer-specific ADC measurements obtained from $ADC_{2\ b\text{-}value}$ and $ADC_{4\ b\text{-}value}$ images

Table 1 summarizes the ADC values measured by Observer 1 using the $ADC_{2\ b\text{-}value}$ and $ADC_{4\ b\text{-}value}$ images for each ROI in brain parenchyma.

Table 2 summarizes the ADC values measured by Observer 2 using the $ADC_{2\ b\text{-}value}$ and $ADC_{4\ b\text{-}value}$ images for each ROI in brain parenchyma.

3.3. Inter-observer reliability analysis of ADC measurements from $ADC_{2\ b\text{-}value}$ and $ADC_{4\ b\text{-}value}$ images

The distribution of ADC measurements from $ADC_{2\ b\text{-}value}$ and $ADC_{4\ b\text{-}value}$ imaging methods between observers is outlined in Fig. 2 and 3.

Both methods showed substantial inter-observer agreement in the distribution of ADC measurements for white matter, thalamus, and globus pallidus. However, for gray matter, there was remarkable difference in the distribution.

Table 3 shows the results of inter-observer reliability estimates for the ADC measurements obtained from $ADC_{2\ b\text{-}value}$ and $ADC_{4\ b\text{-}value}$ images using ICC (Table 3).

Statistical significance test for correlation coefficient was performed on the ADC measurements, and the observed values of the correlation coefficient were 0.0.862 (p = 0.001) for white matter, 0.585 (p = 0.071) for gray matter, 0.767 (p = 0.009) for thalamus, and 0.778 (p = 0.006) for globus pallidus in the $ADC_{2\ b\text{-}value}$ method, while the values were 0.679 (p = 0.029) for white matter, 0.572 (p =

Table 1. Measured Results of ADC Values in ROI of Brain Parenchyma according to $ADC_{2\ b\text{-}value}$ and $ADC_{4\ b\text{-}value}$ Method by Observer 1.

No. of subject \ Parameter	$ADC_{2\ b\text{-}value}$				$ADC_{4b\text{-}value}$			
	White matter	Gray matter	Thalamus	Globus pallidus	White matter	Gray matter	Thalamus	Globus pallidus
1	0.783	0.755	0.779	0.723	0.719	0.741	0.774	0.668
2	0.749	0.711	0.728	0.662	0.668	0.696	0.698	0.624
3	0.794	0.946	0.711	0.749	0.725	0.871	0.687	0.689
4	0.706	0.997	0.716	0.722	0.651	0.864	0.651	0.624
5	0.838	0.761	0.776	0.715	0.737	0.685	0.745	0.641
6	0.820	0.752	0.789	0.696	0.757	0.700	0.770	0.619
7	0.794	0.755	0.734	0.664	0.728	0.722	0.685	0.650
8	0.749	0.820	0.757	0.699	0.691	0.759	0.701	0.649
9	0.749	0.778	0.720	0.797	0.677	0.749	0.719	0.692
10	0.728	0.770	0.767	0.730	0.668	0.747	0.752	0.711
11	0.753	0.825	0.752	0.768	0.719	0.737	0.682	0.734
12	0.861	0.797	0.757	0.727	0.779	0.776	0.702	0.702
13	0.775	0.756	0.731	0.706	0.693	0.701	0.694	0.700

Note. ADC: Apparent Diffusion Coefficient, ROI: Region of Interest, Unit of ADC value: 10^{-3} mm^2/s

Table 2. Measured Results of ADC Values in ROI of Brain Parenchyma according to $ADC_{2\ b\text{-}value}$ and $ADC_{4\ b\text{-}value}$ Method by Observer 2.

Parameter / No. of subject	$ADC_{2\ b\text{-}value}$				$ADC_{4b\text{-}value}$			
	White matter	Gray matter	Thalamus	Globus Pallidus	White matter	Gray matter	Thalamus	Globus Pallidus
1	0.757	0.837	0.781	0.789	0.660	0.807	0.774	0.622
2	0.756	0.863	0.728	0.709	0.682	0.816	0.698	0.602
3	0.754	0.981	0.711	0.696	0.634	0.805	0.757	0.628
4	0.728	0.935	0.661	0.730	0.648	0.852	0.716	0.629
5	0.877	1.050	0.778	0.767	0.758	0.931	0.745	0.723
6	0.813	0.741	0.790	0.743	0.729	0.739	0.770	0.681
7	0.820	0.813	0.741	0.758	0.778	0.802	0.685	0.721
8	0.735	0.896	0.670	0.604	0.678	0.840	0.757	0.678
9	0.772	0.805	0.720	0.735	0.726	0.748	0.719	0.642
10	0.762	0.730	0.787	0.708	0.686	0.694	0.752	0.698
11	0.833	1.045	0.756	0.716	0.731	0.935	0.682	0.734
12	0.920	0.785	0.722	0.756	0.837	0.730	0.757	0.664
13	0.841	0.861	0.735	0.809	0.782	0.743	0.694	0.725

Note. ADC: Apparent Diffusion Coefficient, ROI: Region of Interest, Unit of ADC value: 10^{-3} mm^2/s

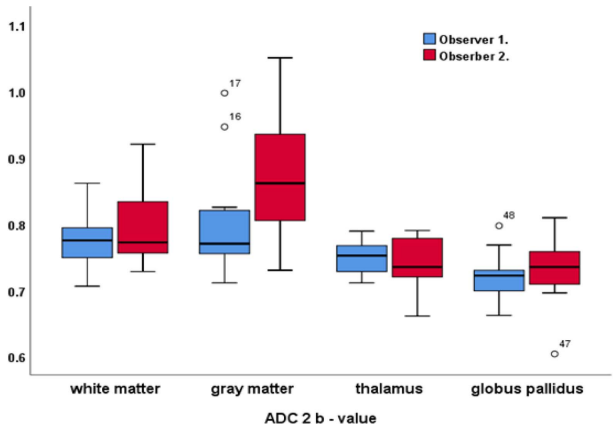

Fig. 2. (Color online) Box and whisker graph shows distribution of apparent diffusion coefficient (ADC) values measured by 2 observer using $ADC_{2\ b\text{-}value}$ method.

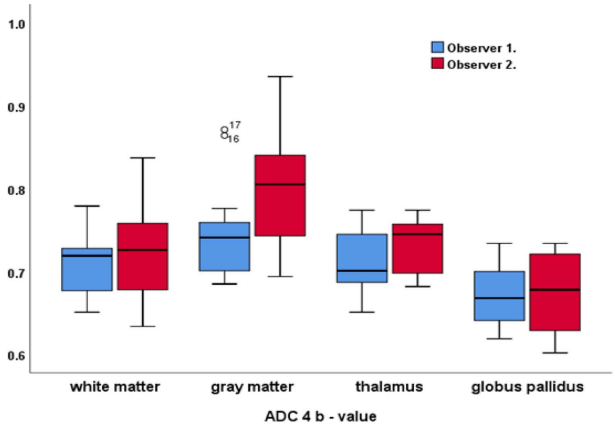

Fig. 3. (Color online) Box and whisker graph shows distribution of apparent diffusion coefficient (ADC) values measured by 2 observer using $ADC_{4\ b\text{-}value}$ method.

0.049) for gray matter, 0.781 (p = 0.006) for thalamus, and 0.717 (p = 0.007) for globus pallidus in the $ADC_{4\ b\text{-}value}$ method.

Both methods showed statistically significant difference and strong correlation between the measured ADC values for white matter, thalamus, and globus pallidus ($p < 0.05$). However, for gray matter, there was a relatively weak correlation, with no significant difference ($p > 0.05$), compared to the other ROIs.

3.4. Significance test for intra-observer variation in ADC measurements obtained from $ADC_{2\ b\text{-}value}$ and $ADC_{4\ b\text{-}value}$ images

Mann Whitney U test was performed to determine whether there is statistically significant variation between the ADC measurements obtained from the $ADC_{2\ b\text{-}value}$ and $ADC_{4\ b\text{-}value}$ images for each observer (Table 4).

For Observer 1, the means and standard deviations of white matter, gray matter, thalamus, and globus pallidus in the $ADC_{2\ b\text{-}value}$ method were 0.777 ± 0.044, 0.802 ± 0.082, 0.747 ± 0.026, and 0.720 ± 0.038, respectively; in the $ADC_{4\ b\text{-}value}$ method, 0.709 ± 0.038, 0.750 ± 0.059, 0.712 ± 0.037, and 0.669 ± 0.037, respectively. Furthermore, the variation in the measured ADC values between the two imaging methods was found to be statistically significant across all ROIs ($p < 0.05$).

For Observer 2, the means and standard deviations obtained from the $ADC_{2\ b\text{-}value}$ method were 0.798 ± 0.059,

Table 3. Results of Inter-Observer Reliability Analysis for ADC Values Measured by Both Imaging Method.

Imaging methods \ Statistical analysis	Inter-Observer Reliability Analysis Using ADC Values				
	ROIs	ICC	95% CIs	*p* value	R^2
$ADC_{2\ b\text{-}value}$	White matter	0.863	0.380 ~ 0.920	0.001	0.721
	Gray matter	0.585	0.361 ~ 0.873	0.071	0.392
	Thalamus	0.768	0.240 ~ 0.929	0.009	0.684
	Globus Pallidus	0.778	0.427 ~ 0.891	0.005	0.678
$ADC_{4b\text{-}value}$	White matter	0.679	0.053 ~ 0.092	0.029	0.690
	Gray matter	0.578	0.267 ~ 0.696	0.050	0.330
	Thalamus	0.785	0.280 ~ 0.934	0.006	0.671
	Globus Pallidus	0.717	0.283 ~ 0.853	0.007	0.622

Note. ADC: Apparent Diffusion Coefficient, ICC: Intraclass Correlation Coefficient, ROI: Region of Interest, CIs: Confidence Intervals. *p* value was less than 0.05.

Table 4. Results of Statistical Analysis of Changed ADC Value between $ADC_{2\ b\text{-}value}$ and $ADC_{4\ b\text{-}value}$ Method Using by Mann Whitney U Test According to Both Observer.

Parameter \ Statistical analysis (n=13)		ADC Value			
		White matter	Gray matter	Thalamus	Globus Pallidus
Observer 1	$ADC_{2\ b\text{-}value}$	0.777 ± 0.044	0.802 ± 0.082	0.747 ± 0.026	0.720 ± 0.038
	$ADC_{4\ b\text{-}value}$	0.709 ± 0.038	0.750 ± 0.059	0.712 ± 0.037	0.669 ± 0.037
	p value	0.001	0.019	0.009	0.003
Observer 2	$ADC_{2\ b\text{-}value}$	0.798 ± 0.059	0.872 ± 0.105	0.737 ± 0.042	0.732 ± 0.051
	$ADC_{4\ b\text{-}value}$	0.718 ± 0.06	0.803 ± 0.074	0.731 ± 0.033	0.673 ± 0.045
	p value	0.005	0.091	0.007	0.004

Note. Data are Mean and ± SD, ADC: Apparent Diffusion Coefficient, Unit of ADC value: 10^{-3} mm^2/s. *p* value was less than 0.05.

0.872 ± 0.105, 0.737 ± 0.042, and 0.732 ± 0.051 for white matter, gray matter, thalamus, and globus pallidus, respectively; and the values obtained from the $ADC_{4\ b\text{-}value}$ method were 0.718 ± 0.06, 0.803 ± 0.074, 0.731 ± 0.033, and 0.673 ± 0.045, respectively, in the same order. The variation in the ADC measurements between the two imaging methods was statistically significant for white matter, thalamus, and globus pallidus ($p < 0.05$), but no statistical significance was found for gray matter ($p > 0.05$). In addition, for both observers, the mean ADC

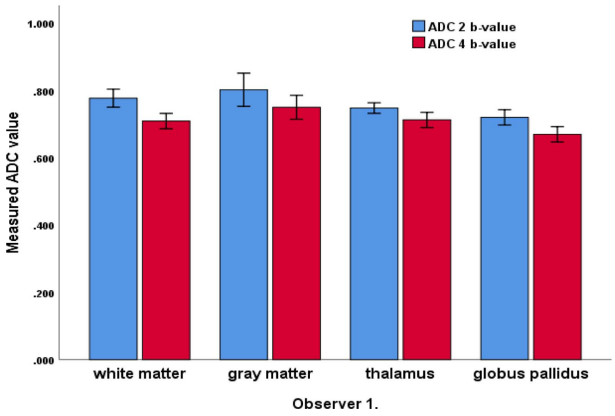

Fig. 4. (Color online) Graph of mean apparent diffusion coefficient (ADC) values for white matter, gray matter, thalamus and globus pallidus respectively using $ADC_{2\ b\text{-}value}$ and $ADC_{4\ b\text{-}value}$ method measured by observer 1. Vertical lines and whiskers denote 95 % CIs.

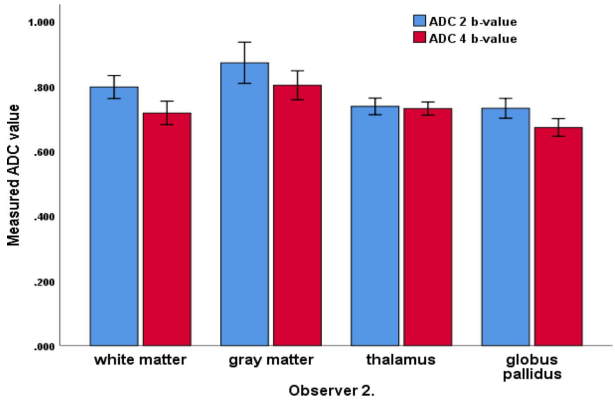

Fig. 5. (Color online) Graph of mean apparent diffusion coefficient (ADC) values for white matter, gray matter, thalamus and globus pallidus respectively using $ADC_{2\ b\text{-}value}$ and $ADC_{4\ b\text{-}value}$ method measured by observer 2. Vertical lines and whiskers denote 95 % CIs.

values measured within ROI in the $ADC_{4\ \text{b-value}}$ method tend to be consistently small, compared to the $ADC_{2\ \text{b-value}}$ method (Fig. 4, 5).

4. Discussion

Diffusion is defined as a state of molecules being in irregular motion due to interaction between their mechanical energy, which is also referred to as Brownian motion. Diffusion results in changes in spatial position of individual molecules.

Diffusion of water molecules in the human body induces phase dispersion to occur in the spinning motion of hydrogen nuclei, consequently leading to a reduction in the MRI signal intensity, even to a slight extent [1]. Based on these phenomena, Stejskal *et al.* [8] introduced an imaging method that involves amplification of small signal difference from diffusion, by addition of diffuse gradient magnetic field before and after 180° RF pulse from spin echo pulse sequence. To achieve this goal, strong gradient magnetic fields are added, pre and post 180° RF pulse, respectively, in the spin echo pulse sequence. According to the basic principle of DW-MRI with strong gradient magnetic fields being applied, the intensity of image signal for diffusion-prone tissues decreases to a large extent as the phase dispersion within a voxel, which is a unit of volume in an image, whereas the signal intensity of the tissues less prone to diffusion decreases, to a relatively small extent. This difference in signal intensity is being used to create images [9]. The degree of diffusion is determined by the integral value of the intensity and time of applied gradient magnetic field, which is referred to as the b-value or gradient factor. As shown below, determination of b-value can be expressed using Equation (3), which includes the following: intensity of the gradient magnetic field (G), the time during which each gradient magnetic field is applied (δ), the time interval between gradient magnetic fields (Δ), and the gyromagnetic ratio (γ)[10].

$$b \text{ value (gradient factor)} = \gamma^2 G^2 \delta^2 \left(\Delta - \frac{\delta}{3}\right) \tag{3}$$

An increase in b-value results in greater difference in phase dispersion of molecules, and diffusion-weighted images can be obtained accordingly. The signal intensity of diffusion-weighted images varies depending on the b-value and the diffusion coefficient (D) of the tissue. Equation (4) shows the variation in the signal intensity of images based on the b-value and the diffusion coefficient of tissue.

$$\ln\left(\frac{SI_{b\ \text{value}}}{SI_0}\right) = -b \text{ value} \cdot D \tag{4}$$

Where SI_0 represents the signal intensity when b-value is equal to 0. In general, water molecules within human body do not exhibit complete diffusion, unlike water molecules in solutions. Restricted diffusion of water molecules takes place in the human body due to physical constraints on molecular movement such as cell membranes and micro-molecules. Thus, the diffusion coefficient of tissue obtained from DW-MRI reflects the restricted diffusion occurring in human tissues, rather than a random molecular motion based on a rigorous definition of diffusion. In addition to the restricted diffusion, other factors such as the movement of tissue, heartbeat, blood flow within the capillaries, and movement of the patients all affect the diffusion coefficient. The coefficient that reflects all these factors is referred to as the apparent diffusion coefficient (ADC) [2, 3, 11].

To measure ADC of a specific tissue, at least two different b-values are needed to obtain DW-MRI images [2, 3]. By using the resulting ADC values on a pixel-by-pixel basis, ADC maps can be created. ADC map image has a unique characteristic where the image contrast is solely determined by the diffusion of water molecules within tissue, with T1, T2 relaxation and proton density effects being ruled out. In ADC map image, tissues with high diffusion coefficient are represented with high intensity signal, while tissues with low diffusion coefficient are represented with low intensity signal [12] (Fig. 6).

DW-MRI and ADC map can quantitatively represent the characteristics of pathological changes in human body using diffusion coefficient, which in turn expands the spectrum of its clinical applications, especially for acute stroke, tumors, and abscesses [13, 14].

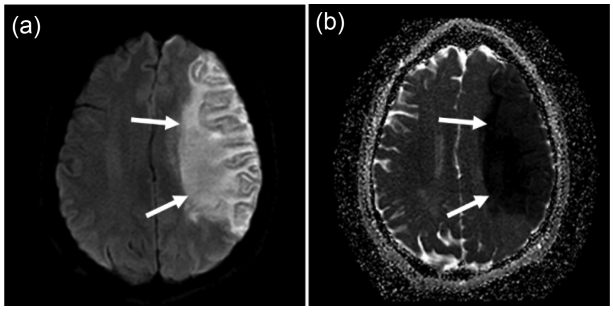

Fig. 6. Strong signal intensity on diffusion weighted image (a) and low signal intensity on ADC map (b) which in low diffusivity lesion (arrow) of acute cerebral infarction patients. Both diffusion weighted image and ADC map were applied with b-value 1000.

Regarding acute stroke, the majority of clinical institutions are obtaining DW-MRI and ADC values using two b-values (0 and 1000) [15, 16]. As described earlier, DW-MRI with a minimum of two b-values is required to obtain the ADC values, which may vary depending on the b-values. In fact, ADC value calculated with lower b-value is greater than the ADC value calculated with higher b-value [17]. Therefore, appropriate selection of b-value must be a priority for the assessment based on ADC values. Moreover, ADC value within the human body does not exhibit monoexponential decay; it exhibits biexponential decay caused by initial perfusion within the tissue. Therefore, even within the same tissue, the ADC values may vary depending on the number of times b-value used. In the previous studies that evaluated ADC values from abdominal organ tissues [6, 7], the use of more b-values was reported to increase the accuracy of ADC value. Similarly, in this study, even for the same ROI in the brain parenchyma, different ADC values were observed between the two imaging techniques using two b-values versus four b-values. Nevertheless, the results showed that ADC value of brain parenchymal tissue was consistently reduced in the method with more b-values ($ADC_{4\ b\text{-}value}$), and the deviation also tended to decrease. This is because the imaging method with more b-values involves, to a greater extent, a biexponential decay pattern. In addition, the inter-observer and intra-observer variations in ADC value were statistically significant ($p < 0.05$). Meanwhile, the variation in ADC value for gray matter showed similar pattern as the other tissues, but no statistically significant difference was found ($p > 0.05$). For gray matter, both observers had difficulty identifying identify clear boundaries of ROI due to ambiguous or uncertain boundary of gray matter both anatomically and on DW-MRI. So, the size of the ROI on gray matter becomes smaller than the other ROIs in the brain parenchymal tissue, which triggers both the partial volume effect caused by the size of voxels and the ghost artifact signals generated from nearby cerebrospinal fluid. Therefore, the measured signals are highly likely to have a wider margin of error. In addition to these findings, the relatively small number of subjects discouraged other considerations from being incorporated into the findings; for example, variation in the ADC values in brain parenchymal tissue due to pathological conditions and underlying diseases or subjects' age distribution, which could be viewed as a limitation of this study.

Measurement of ADC value using DW-MRI is a powerful clinical tool which allows for understanding of pathological progression and treatment outcome using numerical information. From these perspectives, it can be concluded that, ADC value obtained by multiple b-values is a more accurate representation of actual diffusion occurring within the human body. However, this increases the examination time required for imaging, which makes it less practical in many clinical applications. Actual DW-MRI images are susceptible to the microscopic movement of water molecules (diffusion) as well as the voluntary or involuntary macroscopic movement. Therefore, the time required for imaging can be an important factor of ADC value measurement. Furthermore, ADC measurements using DW-MRI are relative values that may vary depending on the subjects' conditions or the hardware system such as imaging equipment performance. All of these aspects should be adequately considered before determining the imaging parameters by b-value.

5. Conclusions

In conclusion, the variation in the ADC values based on two different DW-MRI methods used in this study was found to be statistically significant. Since ADC values of brain parenchyma are relative values in different situations, the number of b-values used should be determined after careful consideration of the time required for imaging and the characteristics of cerebral diseases, rather than unconditionally applying a large number of b-values.

References

[1] L. B. Denis, Magn. Reson. Q **7**, 1 (1991).
[2] D. Chien, K. K. Kwong, D. R. Gress, F. S. Buonanno, R. B. Buxton, and B. R. Rosen, Am. J. Neuroradiol. **13**, 1097 (1992).
[3] S. Warach, D. Chien, W. Li, M. Ronthal, and R. R. Edelman, Neurology **42**, 1717 (1992).
[4] P. W. Schaefer, P. E. Grant, and R. G. Gonzalez, Radiology **217**, 331 (2000).
[5] P. Reimer, P. M. Parzel, and F. A. Stichnoth, Clinical MR Imaging - A Practical Approach, Springer, Verlag Berlin Heidelberg (2003) pp 116-123.
[6] S. Y. Park, C. K. Kim, B. K. Park, and G. Y. Kwon, Am. J. Roentgenol. **203**, 1384 (2014).
[7] C. P. Corona-Villalobos, L. Pan, V. G. Halappa, S. Bonekamp, C. H. Lorenz, J. Eng, and I. R. Kamel, J. Comput. Assist. Tomogr. **37**, 46 (2013).
[8] E. O. Stejskal and J. E. Tanner, J. Chem. Phys. **42**, 288 (1965).
[9] R. Turner, L. B. Denis, J. Maier, R. Vavrek, L. K. Hedges, and J. Pekar, Radiology **177**, 407 (1990).
[10] L. B. Denis, E. Breton, D. Lallemand, P. Grenier, E. Cabanis, and M. Laval-Jeantet, Radiology **161**, 401 (1986).
[11] R. B. Buxton, Principles of diffusion and perfusion MRI,

In R. R. Edelman, J. R. Hesselink, M. B. Zlatkin, Clinical magnetic resonance imaging (2nd eds), Saunders, Philadelphia (1996) pp 233-249.
[12] S. J. Warach, Diffusion and perfusion MRI: functional MRI,In R. R. Edelman, J. R. Hesselink, M. B. Zlatkin, Clinical magnetic resonance imaging (2nd eds), Saunders, Philadelphia (1996) pp 828-835.
[13] P. B. Kingsley and W. G. Monahan, Magn. Reson. Med. **51**, 996 (2004).
[14] A. R. Padhani, G. Liu, D. M. Koh, T. L. Chenevert, H. C. Thoney, T. Takahara, A. Dzik-Jurasz, B. D. Ross, M. V. Cauteren, D. Collins, D. A. Hammoud, G. J. S. Rustin, B. Taouli, and P. L. Choyke, Neoplasia. **11**, 102 (2009).
[15] R. S. Pereira, A. D. Harris, R. J. Sevick, and R. Frayne, J. Magn. Reson. Imaging **15**, 591 (2002).
[16] D. Xing, N. G. Papadakis, C. L. Huang, V. M. Lee, T. A. Carpenter, and L. D. Hall, Magn. Reson. Imaging **15**, 771 (1997).
[17] L. B. Denis, Radiology **268**, 318 (2013).